Available online at www.sciencedirect.com
ScienceDirect
Thin Solid Films 515 (2007) 7625–7628
thin solid films
www.elsevier.com/locate/tsf

Characterization of SiN_x/a-Si:H crystalline silicon surface passivation under UV light exposure

M. Tucci *, L. Serenelli, S. De Iuliis, M. Izzi

ENEA Research Center Casaccia via Anguillarese 301 S. Maria di Galeria, 00123 Roma Italy

Available online 25 January 2007

Abstract

One of the most promising solution for crystalline silicon surface passivation in solar cell fabrication consists in a low temperature (<400 °C) Plasma Enhanced Chemical Vapor Deposition of a double layer composed by intrinsic hydrogenated amorphous silicon (a-Si:H) and hydrogenated amorphous silicon nitride (SiN_x). Due to the high amount of hydrogen in the gas mixture during the double layer deposition, the passivation process results particularly useful in case of multi-crystalline silicon substrates in which hydrogenation of grain boundaries is very needed. In turn the presence of hydrogen inside both amorphous layers can induce metastability effects. To evaluate these effects we have investigated the stability of the silicon surface passivation obtained by the double layer under ultraviolet light exposure. In particular we have verified that this double layer is effective to passivate both p- and n-type crystalline silicon surface by measuring minority carrier high lifetime, via photoconductance-decay. To get better inside the passivation mechanisms, strongly connected to the charge laying inside the SiN_x layer, we have collected the Infrared spectra of the SiN_x/a-Si:H/c-Si structures and we have monitored the capacitance–voltage profiles of Al/SiN_x/a-Si:H/c-Si Metal Insulator Semiconductor structures at different stages of UltraViolet (UV) light exposure. Finally we have verified the stability of the double passivation layer applied to the front side of solar cell devices by measuring their photovoltaic parameters during the UV light exposure.

Keywords: Amorphous material; Silicon nitride; Dielectric properties

1. Introduction

Nowadays industrial silicon solar cells are commonly fabricated using silicon nitride (SiN_x) as passivation layer of the emitter front surface, deposited at low temperature (<400 °C) by Plasma Enhanced Chemical Vapor Deposition (PECDV) system. Even if this silicon nitride is not stoichiometric material (SiN_x), it has provided to perform a very effective antireflection coating and a good degree of silicon surface passivation leading the efficiency of solar cells up to 18% [1,2]. Moreover SiN_x is much more needed to reduce the mechanical stress when thinner and multicrystalline (mc-Si) silicon wafers are adopted [3,4], in order to reduce the cost of energy produced by photovoltaic applications. Recently hydrogenated intrinsic amorphous silicon (a-Si:H) deposited by PECVD has been demonstrated to have excellent passivation quality on both p- and n-type doped silicon substrate. Indeed it has been successfully used either as a buffer layer between SiN_x and the emitter of the cell, leaving antireflection effect almost unchanged, either for the rear side of the cell when a point contact is adopted, reducing the parasitic shunts that occur between inversion layer and local contact on p-type doped silicon based solar cell [5,6]. However, every time hydrogenated materials are involved in device fabrication, metastability problems should be verified. In this paper we analyze the effect of ultraviolet (UV) exposure on passivation quality of SiN_x/a-Si:H stacked layers for both p- and n-type doped silicon. Finally we monitor the stability under UV exposure of the SiN_x/a-Si:H stacked layers deposited on a p-type silicon based solar cells.

2. Experimental

Sample P and N have been fabricated starting on 1 Ω cm<100>oriented CZ monocrystalline silicon wafer p- and n-type doped, having thicknesses of 350 μm and 530 μm respectively. After a standard RCA cleaning procedure the silicon wafers have been introduced in a 13.56 MHz PECVD

* Corresponding author. Tel.: +39 06 3048 4095; fax: +39 06 3048 6405.
E-mail address: mario.tucci@casaccia.enea.it (M. Tucci).

0040-6090/$ - see front matter © 2006 Elsevier B.V. All rights reserved.
doi:10.1016/j.tsf.2006.11.107

Table 1
Structure, C_i, V_{FB}, Q_f, D_{it} of MIS samples before (sample P1 and N1) and after 20 h UV light exposure (sample P2 and N2)

Sample	MIS structure	C_i (nF)	V_{FB} (V)	Q_f/q (cm^{-2})	D_{it} ($cm^{-2}eV^{-1}$)
P1	Al/SiN_x/a-Si:H/p-Si	0.397	−33.5	$1.0 \cdot 10^{13}$	$2.8 \cdot 10^{11}$
P2	Al/SiN_x/a-Si:H/p-Si	0.397	−39	$1.2 \cdot 10^{13}$	$4.2 \cdot 10^{11}$
N1	Al/SiN_x/a-Si:H/n-Si	0.31	−0.5	$1.1 \cdot 10^{11}$	$1.2 \cdot 10^{10}$
N2	Al/SiN_x/a-Si:H/n-Si	0.365	−5.5	$1.6 \cdot 10^{12}$	$1.6 \cdot 10^{10}$

reactor to subsequently deposit on both sides of wafers the a-Si:H and SiN_x with the following parameters respectively: 250 °C as substrate temperature; 0.75 Torr as working pressure; 15 W as RF power; 120 sccm of 5% SiH_4 diluted in Ar. 250 °C as substrate temperature; 0.75 Torr as working pressure; 110 W as RF power; 1.66 as NH_3/SiH_4 gas flow ratio. These samples have been characterized by photo-conductance decay to estimate the minority carrier effective lifetime τ_{eff}, and by Infrared (IR) spectroscopy. Then they have been cut in two (P1, P2, N1, N2) in order to take P1 and N1 as reference not UV exposed. τ_{eff} has been monitored at different times of the UV exposure on sample P2 and N2. The UV light has been obtained by a deuterium lamp, filtered to reduce the spectrum to UV-A region, and focused to obtain a power density of 500 μW/cm^2.

To get more inside the behavior of the passivation layers, Metal Insulator Semiconductors (MIS) structure have been fabricated on the described samples as reported in Table 1. These MIS have been characterized by capacitance–voltage (C–V) and conductance–voltage (G–V) measurements, performed in dark and room temperature conditions, in the range of 0.1–10 KHz frequency and ±40 V gate voltage. From these measures several data have been estimated: the flat band voltage V_{FB} from C–V profile [7,8]; the charge within the insulator Q_f from the V_{FB} [8]; the interface trap density D_{it} from G–V measurements [9].

Finally the experimented double layer passivation has been deposited on top of a p-type doped silicon based solar cell described elsewhere [10], having a Ti/Pd/Ag top metal grid.

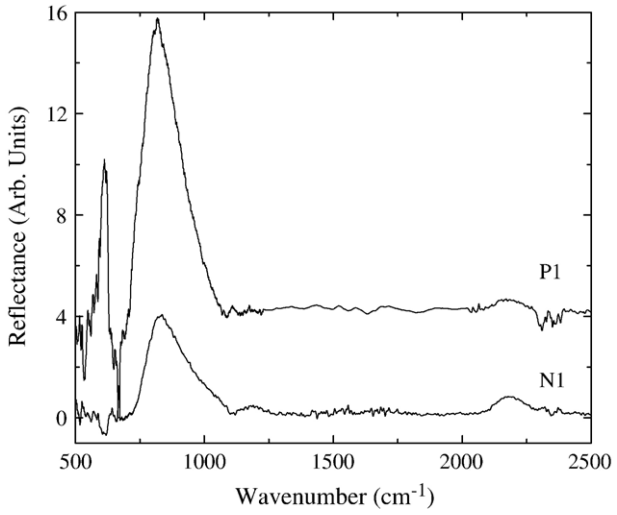

Fig. 1. IR spectra of sample P1, N1 measured before UV light exposure.

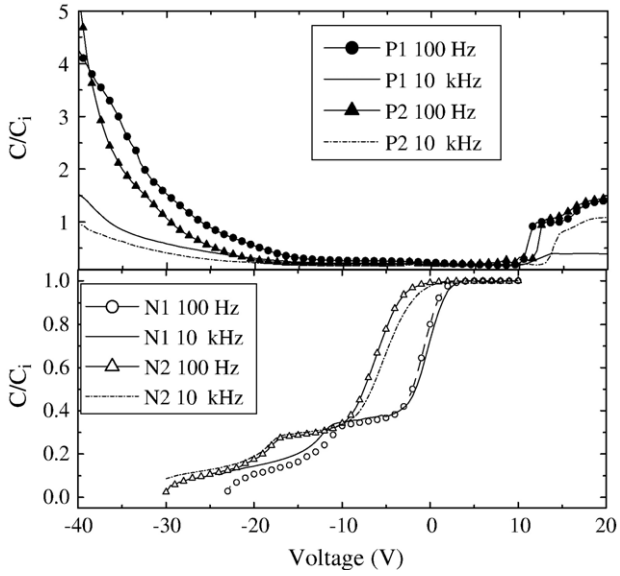

Fig. 2. C–V measurements at 100 Hz and 10 KHz of samples P1 and N1 before UV light exposure and samples P2 and N2 after 20 h UV light exposure.

These solar cell has been characterized at different stage of UV exposure by current–voltage measurements (I–V) at room temperature in dark and AM1.5G, collecting the photovoltaic parameters such as short circuit current density (J_{sc}), open circuit voltage (V_{oc}), fill factor (FF) and efficiency (Eff).

3. Results and discussion

In Fig. 1 the IR spectra of sample P1 and N1 before UV irradiation are reported. Comparing these spectra is evident that the peaks at 820 cm^{-1}, 614 cm^{-1}, 1550 cm^{-1}, related to N–Si_3 (asymmetric stretching mode [11]), Si–Si (stretching mode [12]), NH_2 (wagging mode [13]) respectively are higher in sample P; while the 2170 cm^{-1}, relative to H–Si–HN_2 (stretching mode [14]) are higher in sample N1. Therefore it is evident that the SiN_x/a-Si:H double layer composition depends on the doping type of silicon substrates on which it has been grown. It is important to point out that the introduction of a-Si:H buffer layer between SiN_x and Si is able to produce an increase of up to one order of magnitude of the τ_{eff} with respect to the single SiN_x passivation layer on both doping type of substrates. Although the measured effective lifetime is not the optimum for 1 Ω cm silicon, it is very good for a low temperature passivation.

In Fig. 2 the C–V profiles normalized to the insulator capacitance C_i (listed in Table 1) for sample P1 and N1 are reported. These curves describe a step function from depletion to accumulation positioned on the flat band voltage (V_{FB}). The distortion of the step function can be related to voltage stretch-out with interface trap charge distribution. Different positions in the capacitance step function can be found, depending on the probe frequency. On both p- and n-type doped silicon a shift of V_{FB} toward negative values occurs with respect to an ideal value, revealing the presence of fixed positive charge Q_f. This can be evaluated taking into account the accumulation regime or by means of thickness of the insulator as in sample P1 and P2.

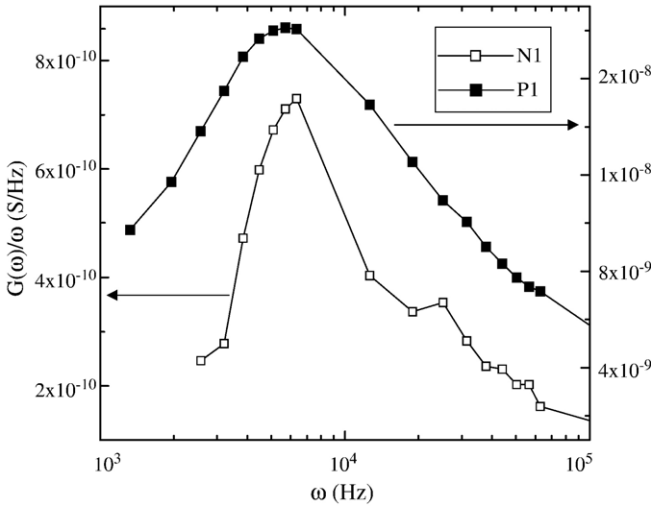

Fig. 3. $G(\omega)/\omega$ vs ω of samples P1 and N1.

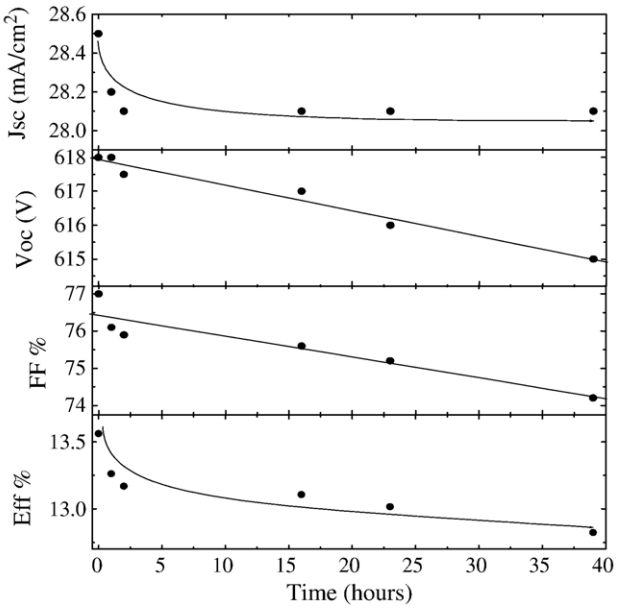

Fig. 5. Evolution of photovoltaic parameters during UV light exposure.

This charge is commonly attributed to silicon dangling bonds which consist of a silicon atom bonded to three nitrogen atoms, having an unpaired electron [15,16]. The presence of this positive charge within the SiN_x produces a different passivation mechanism depending on the doping type of substrate. On p-type doped silicon (sample P1) electrons are attracted close to the interface and an inversion layer occurs that becomes evident when a $C–V$ profile is performed at low frequency. Instead in sample N1, the positive charge attracts electrons close to the silicon surface, enhancing the accumulation. Therefore the inversion layer does not appear, neither when a low frequency probe is applied and the accumulation regime still remains when the MIS is biased at negative gate voltage.

The passivation of silicon surface is affected by the presence of interface states arising from plasma deposition of the amorphous layers related to dangling bonds at the interface and hydrogen diffusion into the silicon substrate [17]. An evaluation of their amount and energy position in the gap can be obtained by $G–V$ measurements. The plot of $G(\omega)/\omega$, reported in Fig. 3 for sample N1, shows a peak, weak bias dependent in amplitude, positioned at 1 kHz that does not vary with the gate voltage. This reveals that:

1) a level of trap lays at energy position $E=KT\cdot\ln(\nu/\omega)$ of 0.37 eV from the valence band within the silicon band-gap, calculated assuming an escape frequency of $\nu = 10^{10}$ for c-Si;
2) the level extends inside the silicon substrate at the same energy reducing its density and the Fermi level crosses it always at the same distance from the depletion edge.At the

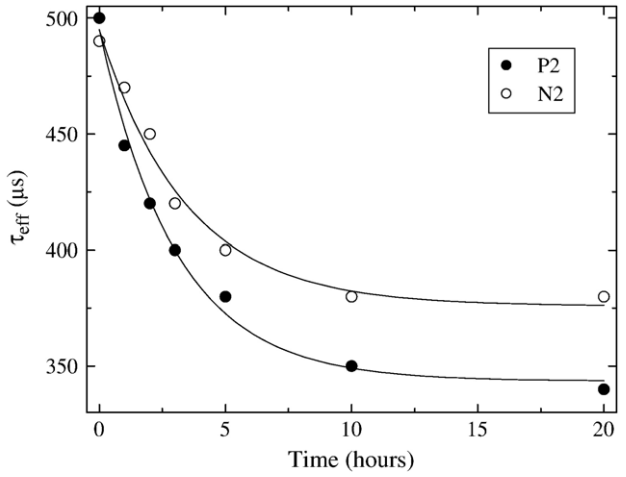

Fig. 4. Effective minority carriers lifetime τ_{eff} of sample P2 and N2 at different time of UV light exposure.

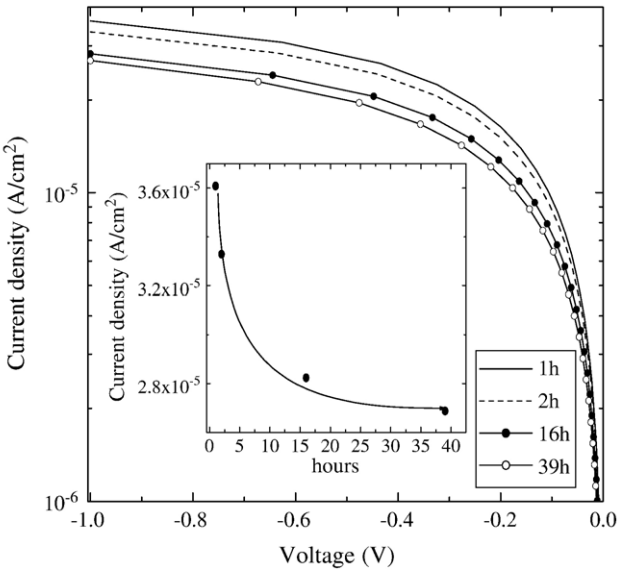

Fig. 6. $I–V$ characteristics in reverse bias and dark conditions at different time of UV light exposure. In the inset, the current density at −1 V of bias is reported as a function of exposure time.

a-Si:H/Si interface this trap level assumes the highest density (D_{it}), that can be calculated directly from the maximum of $G(\omega)/\omega$ [9]. This trap reduces the possibility of an inversion layer at the silicon surface, since the Fermi level cannot easily move beyond the energy of that trap level toward the valence band edge. Moreover if holes are attracted at the silicon surface they can be trapped and released into the amorphous silicon band tail, leading to a new broaden distribution of $G(\omega)/\omega$. Sample P1 in depletion regime shows a higher peak positioned at 1 kHz, that still remains evident in inversion regime, confirming that it exchanges with electrons. Moreover when the sample P1 is in accumulation a trap of holes within the a-Si:H band tail occurs, corresponding again to a broadening of $G(\omega)/\omega$. Therefore the D_{it}, summarized in Table 1, are calculated always at a gate bias at which the Fermi level crosses 0.37 eV.

The UV light exposure of the double insulator layer affects the total amount of charge and traps. Indeed the C–V profiles, performed after 20 h of UV light exposure and reported in Fig. 2, show that V_{FB} of both samples P2 and N2 shifts toward more negative values, revealing an increment of positive charge. Hence, the traps that have been induced during plasma deposition at interface with the silicon wafer, can be enhanced by UV radiation, producing a rise of the $G(\omega)/\omega$ at 1 kHz. In Table 1 the V_{FB}, Q_f and D_{it} of sample P2 and N2 after 20 h of UV light exposure are summarized. From these data is evident that higher is the increment of positive charge, lower is the traps effect on the surface recombination velocity, leading to a better stability of passivation of silicon surface, as evident in sample N2 by the τ_{eff} decay reported in Fig. 4. Since different passivation mechanism occurs on p- and n-type silicon, this increment of charge does not necessarily lead to the same result of course.

Furthermore a comparison of IR spectra before and after UV light exposure does not show significant difference.

Finally SiN_x/a-Si:H passivation layer has been deposited over the emitter layer of a solar cell, producing an increase of its photovoltaic parameters due to passivation and antireflection effects. In particular the V_{oc} increases from 598 mV up to 618 mV. Even though SiN_x layer is dimensioned as antireflection coating, the a-Si:H layer absorbs a slight part of blue region of the sun spectrum, slightly reducing the J_{sc}. The enhancement of V_{oc} also confirms the efficacy of the SiN_x/a-Si:H as passivation layer on an n-type emitter. During the UV light exposure, the photovoltaic parameters show different behavior as depicted in Fig. 5. While V_{oc} remains almost unchanged, J_{sc} decreases by 1.4% and FF decreases by 3% and then the efficiency loses an absolute 0.5%. This effect is mainly due to the increase of defects at a-Si:H/Si interface that enhances the surface recombination, as confirmed by the reverse bias I–V characteristics in the dark reported in Fig. 6, as well as the reduction of τ_{eff}. Indeed if at a-Si:H/Si interface the density of traps increases, a reduction of minority carriers occurs and then a decrease of injected current in reverse bias takes place. In the inset of Fig. 6 the current density collected at −1 V of bias is reported as a function of UV exposure time. A decay of about 20% of current density occurs very similar to that of τ_{eff} of sample N2 seen in Fig. 4.

4. Conclusion

In this paper the mechanism of silicon surface passivation imposed by SiN_x/a-Si:H double layer has been evaluated for both doping type of crystalline silicon and has monitored during the UV light exposure. IR spectroscopy has been shown that the bonding composition of passivation layer depends on doping type of silicon substrate. Impedance measurements have confirmed the role of positive charge in the passivation mechanism of both doping type of silicon substrate and have been established that UV light exposure produces an increment of both positive charge and interface traps. During UV light exposure the passivation of silicon surface obtained by SiN_x/a-Si:H layer has degraded less when this layer has been deposited on n-type rather than grown on p-type silicon. Finally SiN_x/a-Si:H has been resulted in an effective passivation layer and antireflection coating of a p-type based solar cell. The UV light exposure of this cell has produced an efficiency loss of 0.5%, due to the increment of traps close to the a-Si:H/Si interface.

References

[1] T. Lauinger, J. Moschner, A.G. Aberle, R. Hezel, J. Vac. Sci. Technol., A 16 2 (1998) 530.
[2] A.G. Aberle, Sol. Energy Mater. Sol. Cells 65 (2001) 239.
[3] M.A. Green, A.W. Blakers, J. Zhao, A.M. Milne, A. Wang, X. Dai, IEEE Trans. Electron Devices 37 (1990) 331.
[4] H. Nagel, J. Schmidt, A.G. Aberle, R. Hezel, Proceedings of the 20th European Photovoltaic Solar Energy Conference, Barcelona, Spain, June 6–10, 2005, p. 762.
[5] H. Plagwitz, M. Schaper, A. Wolf, R. Meyer, J. Schmidt, B. Terheiden, R. Brendel, Proceedings of the 20th European Photovoltaic Solar Energy Conference, Barcelona, Spain, June 6–10, 2005, p. 725.
[6] M. Schaper, J. Schmidt, H. Plagwitz, R. Brendel, Prog. Photovolt.: Res. Appl. 13 (2005) 381.
[7] R.J. Hillard, J.M. Heddleson, D.A. Zier, P. Rai-Choudhury, D.K. Schroder, Diagn. Tech. Semicond. Mater. Devices, Electrochem. Soc. (1992) 261.
[8] D.K. Schroeder, Semiconductor Material Device Characterization, Wiley Interscience, New York, 1998 Cap. 6.
[9] E.H. Nicollian, J.R. Brews, MOS: Physics and Technology, J. Wiley & Son, New York, 1982 Cap.7.
[10] L. Serenelli, S. De Iuliis, M. Izzi, G. Arabito, M. Tucci, D. Caputo, G. de Cesare, A. Nascetti, Proceedings of the 20th European Photovoltaic Solar Energy Conference, Barcelona, Spain, June 6–10, 2005, p. 1232.
[11] G. Lucovsky, R.J. Nemanich, J.C. Knight, PHys. Rev., B, Condens. Matter Mater. Phys. 19 (1979) 2064.
[12] B.S. Sahu, A. Kapoor, P. Srivastava, O.P. Agnihotri, S.M. Shivaprasad, Semicond. Sci. Technol. 18 (2003) 670.
[13] G.N. Parsons, J.H. Souk, J. Batey, J. Appl. Phys. 70 (3) (1991) 1553.
[14] Y. Masaki, R.A.G. Gibson, P.G. Lecomber, J. Appl. Phys. 73 (10) (1993) 5088.
[15] L. Zhong, F. Shimura, Appl. Phys. Lett. 62 (6) (1993) 615.
[16] W.L. Warren, P.M. Lenahan, J. Kanicki, J. Appl. Phys. 70 (4) (1991) 2220.
[17] M. Tucci, E. Salurso, F. Palma, Thin Solid Films 403–4 (2002) 307.